# A Nonlocal Density Functional Study of the Pd(II)-Assisted Copolymerization of Ethylene and CO

**Peter Margl and Tom Ziegler***

*Contribution from the Department of Chemistry, University of Calgary, 2500 University Drive, N.W., T2N 1N4 Calgary, Alberta, Canada*

*Received March 4, 1996. Revised Manuscript Received June 3, 1996*[⊗]

**Abstract:** We study the homogeneous catalytic copolymerization of olefin and carbon monoxide.[1−4] The catalytic center is modeled by Pd(II) coordinated to $PH_2CH{=}CHPH_2$. $C_2H_4$ is used as a model for the olefin. We investigate the chain propagation mechanism for alternating copolymerization as well as the side reactions resulting from multiple insertion of olefin and CO, respectively. We find that strictly alternating copolymerization is kinetically favored over homopolymerization of olefin and thermodynamically as well as kinetically favored over successive multiple insertions of CO. Insertion of one $C_2H_4$−CO unit into the Pd−ethyl bond yields −219 kJ/mol, whereas insertion of a $C_2H_4$−$C_2H_4$ segment yields exactly −200 kJ/mol. Insertion of a CO−CO segment yields only −88 kJ/mol. Therefore, multiple successive CO insertions are by comparison so unfavorable as to be ruled out completely. We explain the experimentally observed preference of strictly alternating copolymerization over multiple olefin insertions by the higher adduct formation energy of CO (−78 kJ/mol) as opposed to only −51 kJ/mol for $C_2H_4$. Furthermore, the activation barriers for the insertion of a CO/$C_2H_4$ unit into the chain are only 48 and 58 kJ/mol, respectively, whereas the barrier for $C_2H_4$ insertion is 65 kJ/mol. All acyl species encountered are only weakly stabilized by agostic interactions, whereas Pd-alkyl species are strongly stabilized by agostic interactions. The acyl species can stabilize itself by −31 kJ/mol over the most favorable agostic conformation by adopting a $\eta^2$-carbonyl conformation. The growing polyketone chain is strongly stabilized by forming chelate bonds between the carbonyl oxygens and Pd. The strictly alternating copolymerization pattern originates from a combination of effects: On the one hand, the number of CO units incorporated into the chain is maximized, because CO (as the better $\pi$ acceptor) stabilizes the reactive center more than ethylene during the adduct formation proceeding insertion and CO also faces a lower barrier during insertion into the chain. On the other hand, subsequent multiple insertions of CO are avoided since they are kinetically as well as thermodynamically highly unfavorable.

## 1. Introduction

Olefin−CO copolymers (polyketones) are considered to be of great technical importance[1,3−10] due to the useful properties introduced into the polymer chain by the presence of keto groups. The carbonyl groups can be efficiently modified to introduce new functionalities into the polymer and make the polymer photodegradable. Due to recent advances in the synthesis of olefin−CO copolymers, it is now possible to synthesize chiral copolymers with the use of homogeneous catalysts such as those proposed by Jiang and Sen[5] where the chiral copolymer is built up out of prochiral constituents. The mechanistic details of the copolymerization reaction are well established (Figure 1),[5,9] but no theoretical investigation has been performed to elucidate its energetics and kinetics.

It is our goal here to apply density functional theory to shed light on the mechanistic details of the copolymerization of CO and olefin. We model the growing polymer chain as composed of CO and ethylene. The catalytic center consists of Pd(II) coordinated by $H_2PCH{=}CHPH_2$ (Chart 1b), which is used to model the chiral Me-DUPHOS (Chart 1a) ligand of the original study by Sen.[5] In the present study, we focus exclusively on the generic aspects of the copolymerization process, putting aside the question of stereoselectivity. Therefore, we chose $H_2PCH{=}CHPH_2$ as a model ligand since it preserves all the features which the Me-DUPHOS ligand imparts on the reaction, except the ability to induce chirality in the growing chain. The additional bulky groups in Me-DUPHOS can be thought of as adding a (small) perturbation to the generic energy surface. Once the shape of the generic energy surface is known, this perturbation can easily be incorporated using combined QM-MM techniques which treat steric bulk by effective Van der Waals potentials.

The usually accepted reaction mechanism for the CO/olefin copolymerization calls for the precatalyst (in our case $Pd^{II}H_2PCH{=}CHPH_2^{2+}$, in the following referred to as PdPP) to be activated, f.i. by $\beta$-hydrogen abstraction from a Pd-alkoxy species formed from the precatalyst and solvent alcohol or by a water−gas shift reaction of trace water in otherwise aprotic media,[5,9] resulting in a Pd(II) hydride species ($PdPPH^+$, **1**). **1** can add an olefin, directly forming $PdPPC_2H_5^+$ (**3**). To form an alternating copolymer, **3** adds CO, which is inserted into the Pd−$C_2H_5$ bond to form the Pd-acyl **7**, which in turn can add and insert an olefin, thus propagating the chain. The regularity of the polymer can be impaired by a misinsertion of CO (Figure 2) or olefin (Figure 3), which would yield an irregular block copolymer.

However, it seems that misinsertion of olefin and/or CO are extremely rare phenomena under conditions which also permit alternating copolymerization. Additionally, it seems puzzling that despite these systems' demonstrated ability to efficiently

[⊗] Abstract published in *Advance ACS Abstracts,* July 15, 1996.

(1) Drent, E.; Budzelaar, P. H. M. *Chem. Rev.* **1996**, *96*, 663.
(2) Sen, A.; Lai, T.-W. *J. Am. Chem. Soc.* **1982**, *104*, 3520.
(3) Sen, A.; Jiang, Z. *Macromolecules* **1993**, *26*, 9111.
(4) Drent, E.; Broekhoven, J. A. M. v.; Doyle, M. J. *J. Organomet. Chem.* **1991**, *417*, 235.
(5) Jiang, Z.; Sen, A. *J. Am. Chem. Soc.* **1995**, *117*, 4455.
(6) Lain, T.-W.; Sen, A. *Organometallics* **1984**, *3*, 866.
(7) Valli, V. L. K.; Alper, H. *J. Polym. Sci. A* **1995**, *33*, 1715.
(8) Kacker, S.; Sen, A. *J. Am. Chem. Soc.* **1995**, *117*, 10591.
(9) Sen, A. *Acc. Chem. Res.* **1993**, *26*, 303.
(10) Lai, T.-W.; Sen, A. *Organometallics* **1984**, *3*, 866.

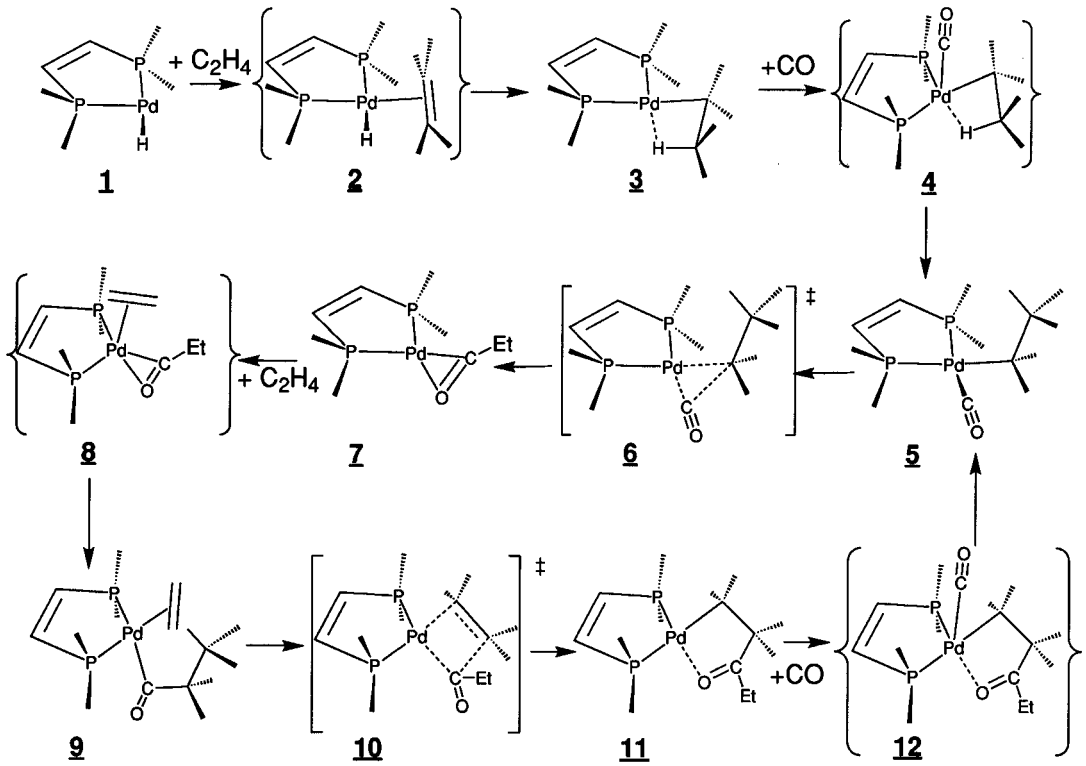


**Figure 1.** Flow chart of the productive section of the catalytic cycle leading to an alternating CO/olefin copolymer. Stages of the reaction are identified with numbers. Species in square brackets with ‡ superscript refer to transition states, and structures in curved brackets refer to unstable (not observable) species. All species referred to in this work carry a single positive charge.

**Chart 1**

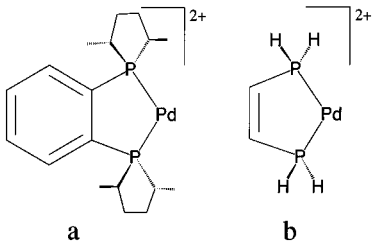


homopolymerize olefins,[11] no polyolefin is formed under conditions which also allow copolymerization with CO. No theoretically founded explanation for this has yet been given, although it is generally assumed that CO misinsertion is energetically unfavorable and thus not observed. An explanation as to why no successive multiple insertions of olefin are observed is not straightforward. It is the aim of this work to explain the experimentally observed overwhelming preference of alternating insertion over successive multiple insertions of either olefin or CO on a first-principles basis, using density functional theory as embodied in the ADF program.

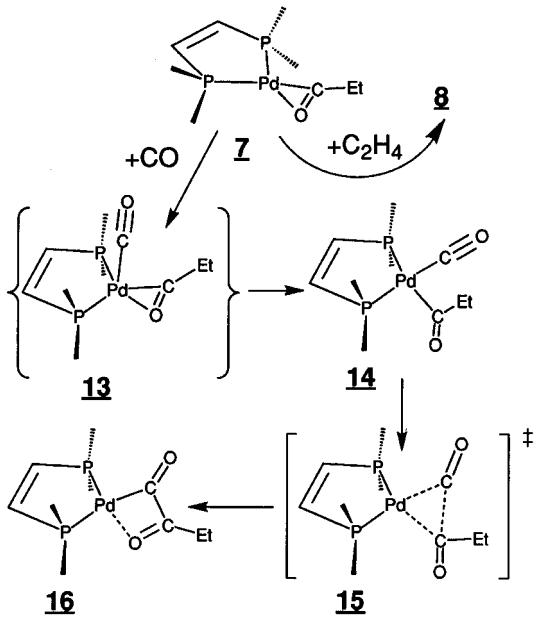


**Figure 2.** Flow chart of the CO misinsertion during the catalytic copolymerization of CO and olefin. CO misinsertion branches off the productive cycle at stage **7** (see also Figure 1).

## 2. Computational Details

Stationary points on the potential energy surface were calculated with the program ADF, developed by Baerends *et al.*,[12,13] and vectorized by Ravenek.[14] The numerical integration scheme applied for the calculations was developed by te Velde *et al.*[15,16] The geometry optimization procedure was based on the method due to Versluis[17] and Ziegler. The electronic configurations of the molecular systems were described by a triple-ζ basis set on palladium[18−20] for 4s, 4p, 4d, 5s, and 5p. Double-ζ STO basis sets were used for carbon (2s, 2p), hydrogen (1s), phosphorus (3s, 3p), and oxygen (2s, 2p), augmented

(11) Johnson, L. K.; Killian, C. M.; Brookhart, M. *J. Am. Chem. Soc.* **1995**, *117*, 6414.
(12) Baerends, E. J. Ph.D. Thesis, Free University, Amsterdam, The Netherlands, 1973.
(13) Baerends, E. J.; Ellis, D. E.; Ros, P. *Chem. Phys.* **1973**, *2*, 41.
(14) Ravenek, W. In *Algorithms and Applications on Vector and Parallel Computers*; te Riele, H. J. J., Dekker, T. J., van de Horst, H. A., Eds.; Elsevier: Amsterdam, The Netherlands, 1987.
(15) te Velde, G.; Baerends, E. J. *J. Comput. Chem.* **1992**, *99*, 84.
(16) Boerrigter, P. M.; te Velde, G.; Baerends, E. J. *Int. J. Quantum Chem.* **1988**, *33*, 87.
(17) Versluis, L.; Ziegler, T. *J. Chem. Phys.* **1988**, *88*, 322.
(18) te Velde, G. *ADF 1.1.3 User's Manual*; Vrije Universiteit Amsterdam, 1994.
(19) Snijders, J. G.; Baerends, E. J.; Vernoijs, P. *At. Nucl. Data Tables* **1982**, *26*, 483.
(20) Vernoijs, P.; Snijders, J. G.; Baerends, E. J. *Slater Type Basis Functions for the Whole Periodic System*; Internal report (in Dutch); Department of Theoretical Chemistry, Free University: Amsterdam, The Netherlands, 1981.

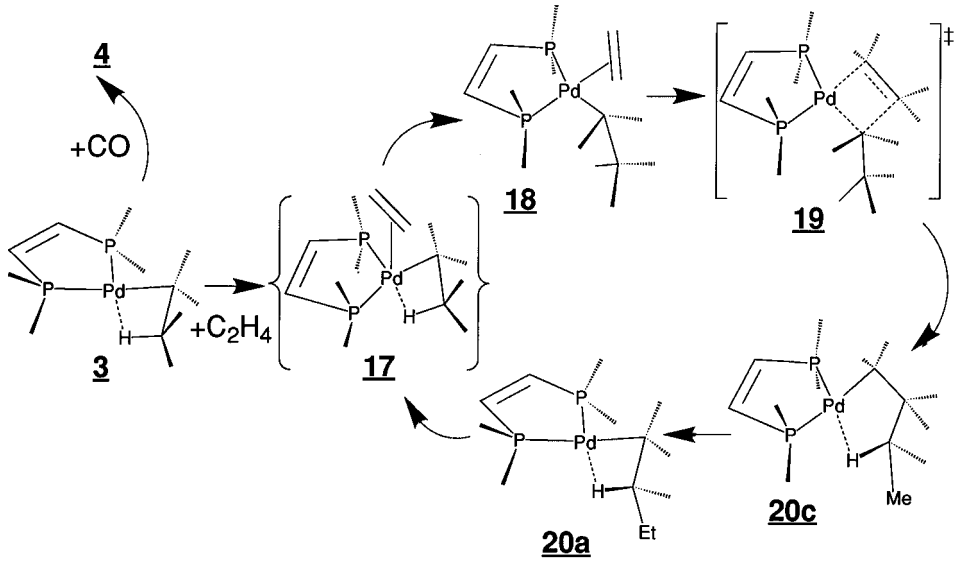


**Figure 3.** Misinsertion of olefin during the catalytic copolymerization of CO and olefin. Olefin misinsertion branches off the productive cycle at stage **3** (see also Figure 1).

with a single 3d polarization function except for hydrogen where a 2p function was used. The $1s^2 2s^2 2p^6 3s^2 3d^{10}$ configuration on palladium, the $1s^2$ shell on carbon and oxygen, as well as the $1s^2 2s^2 2p^6$ shells on phosphorus were assigned to the core and treated within the frozen core approximation.[13] A set of auxiliary[21] s, p, d, f, and g STO functions, centered on all nuclei, was used in order to fit the molecular density and present Coulomb and exchange potentials accurately in each SCF cycle. Energy differences were calculated by including the local exchange-correlation potential by Vosko *et al.*[22] with Becke's[23] nonlocal exchange corrections and Perdew's[24,25] nonlocal correlation correction. Geometries were optimized including nonlocal corrections. First-order scalar relativistic corrections[26−28] were added to the total energy, since a perturbative relativistic approach is sufficient for 4d metals. Since all systems investigated in this work show a large HOMO-LUMO gap of at least 2 eV, a spin-restricted formalism was used for all calculations. No symmetry constraints were used, except where explicitly indicated. Saddle-point determinations were initialized by a linear transit search from reactant to product along an assumed reaction coordinate. In each step along the reaction coordinate all other degrees of freedom were optimized. Full transition state optimizations were carried out on the geometries obtained by linear transit.

## 3. Results and Discussion

**(a) The Productive Cycle.** The catalytic cycle is initiated with the formation of the palladium hydride **1**. As expected from the fact that **1** is a $d^8$ system and from previous theoretical work,[29,30] the hydride assumes a position trans to one of the phosphorus atoms in a square-planar conformation with a single vacant site.

Attempts to locate an energy minimum representing the ethene complex PdPP(H)($C_2H_4$) (**2**, Figure 1) by geometry optimization led invariably directly to the $\beta$-agostic ethyl compound **3a**. This would indicate that **1** directly incorporates a free olefin to form the $\beta$-agostic ethyl **3a** without generating

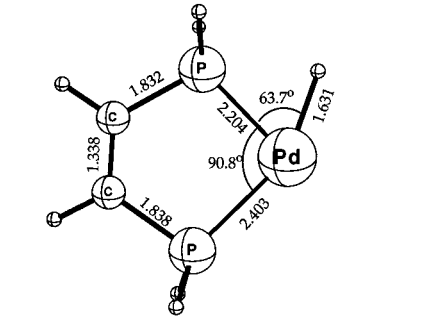


**1**

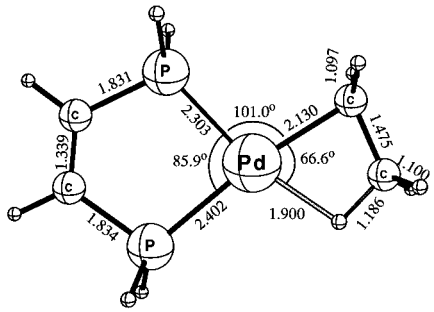


**3a**

a stable $\pi$-complex (**2**) as an intermediate. A direct ethylene insertion is not unusual for many types of transition metal hydrides and has been observed in a number of cases.[29] The reaction **1** + $C_2H_4$ → **3a** is exothermic by −177 kJ/mol (Figure 4), which is in agreement with previous theoretical results.[29] Both structures **1** and **3a** assume planar ($C_s$ symmetric) geometries, although $C_s$ symmetry was not explicitly enforced during the optimization. The T-shaped and square-planar conformations are known to be the most stable geometries for 3- and 4-coordinate $d^8$ compounds of this type. We estimate the $\beta$-agostic bond in **3a** to have a strength of 44 kJ/mol. This estimate was obtained by comparing the energy of **3a** to that of an optimized structure **3b** in which the $\beta$-hydrogen has been moved out of the plane by a rotation of 65° around the Pd−$C_\alpha$ bond. The value of 44 kJ/mol represents a lower limit for the bond strength, since the $\beta$-agostic interaction in **3a** is replaced by a weaker α-agostic one in **3b**.

The formation of an alternating copolymer requires that **3** captures a CO molecule and inserts it into the Pd−$C_\alpha$ bond.

(21) Krijn, J.; Baerends, E. J. *Fit Functions in the HFS Method*; Internal Report (in Dutch); Department of Theoretical Chemistry, Free University: Amsterdam, The Netherlands, 1984.
(22) Vosko, S. H.; Wilk, L.; Nusair, M. *Can. J. Phys.* **1980**, *58*, 1200.
(23) Becke, A. *Phys. Rev. A* **1988**, *38*, 3098.
(24) Perdew, J. P. *Phys. Rev. B* **1986**, *34*, 7406.
(25) Perdew, J. P. *Phys. Rev. B* **1986**, *33*, 8822.
(26) Ziegler, T.; Tschinke, V.; Baerends, E. J.; Snijders, J. G.; Ravenek, W. *J. Phys. Chem.* **1989**, *93*, 3050.
(27) Snijders, J. G.; Baerends, E. J. *Mol. Phys.* **1978**, *36*, 1789.
(28) Snijders, J. G.; Baerends, E. J.; Ros, P. *Mol. Phys.* **1979**, *38*, 1909.
(29) Fan, L.; Krzywicki, A.; Somogyvari, A.; Ziegler, T. *Inorg. Chem.* **1994**, *33*, 5287.
(30) Fan, L.; Krzywicki, A.; Somogyvari, A.; Ziegler, T. *J. Am. Chem. Soc.* Submitted for publication.

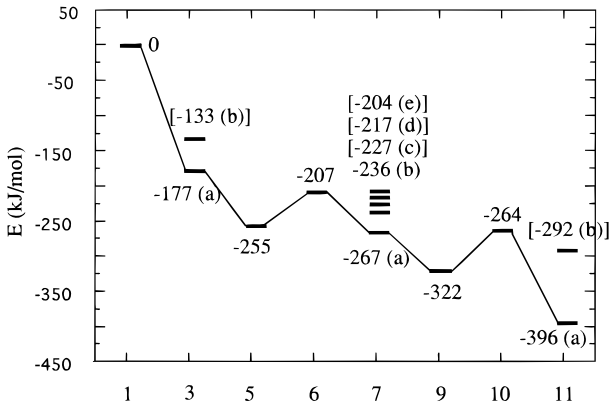


**Figure 4.** Energy profile for the productive part of the catalytic copolymerization of CO and $C_2H_4$. Energies in kJ/mol. Stages of the reaction are identified with numbers (see Figure 1), and energies of free monomers are included. Different isomers of a given species are distinguished with alphanumerics. Isomer energies obtained from a geometry constrained calculation are given in square brackets.

Since the fourth ligand position of the square-planar complex **3a** is occupied by an agostic bond, the CO molecule can be added to one of the free apical positions of **3**. The resultant 5-coordinate complex **4** (Figure 1) was found not to constitute a stationary point on the potential surface. Instead, it relaxed during a geometry optimization without a barrier into the 4-coordinate square-planar compound **5**, in which the ethyl group has been rotated around the Pd−$C_\alpha$ axis and the agostic bond is broken. The exothermicity of this step is −78 kJ/mol, which is in the range expected for a CO uptake reaction.[31,32]

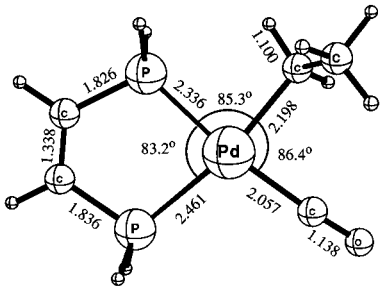


**5**

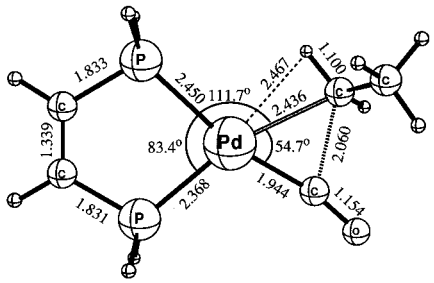


**6**

The transition state for the CO insertion, **6**, lies only 48 kJ/mol above the resting state **5**. This activation energy is rather low compared to the calculated barrier for migratory insertion of CO into a transition metal−alkane bond[33−36] in other systems. We have previously argued[35] that the barrier increases with the amount of density back-donated from the metal into the $\pi^*_{CO}$ LUMO of the CO ligand involved in the migratory insertion. In the present case with a positively charged metal center the back-donation is modest, and hence the barrier relatively low.

At the transition state geometry, the α-carbon of the ethyl group orients its local $C_3$-axis ($sp^3$ $\sigma$ orbital) toward the carbonyl carbon atom to establish an interaction with a $\pi^*_{CO}$ orbital of the carbonyl group.[33,35] We also note that at the transition state, the α-agostic stabilization provided by the ethyl group is very weak (agostic bond distance ≈2.5 Å), due to a shift in electron density toward the carbonyl group which results in a depletion of electron density from the agostic hydrogen. In both **5** and **6**, the atoms coordinating to palladium show no significant deviation from square-planar arrangement.

The resulting acyl complex **7b** lies 19 kJ/mol above the educt **5**. The acyl complex is able to undergo $\gamma$- and $\beta$-agostic interactions with the metal atom. We have investigated three possible agostic conformations, namely the $\eta^1$-$\beta$- (**7b**, 19 kJ/mol above **5**), the $\eta^2$-$\gamma$- (**7d**, +38 kJ/mol, $C_s$ symmetry constraint), and the $\eta^1$-$\gamma$-agostic (**7e**, +51 kJ/mol, $C_s$ symmetry constraint) structures. The agostic interactions in **7b,d,e** are very weak, as their agostic Pd−H distances are ≈2.5 Å. We estimate the $\beta$-agostic bond in **7b** to have a strength of 9 kJ/mol. This estimate was obtained by comparing the energy of **7b** to that of an optimized structure in which the $\beta$-hydrogen has been moved out of the plane by a rotation of 90° around the Pd−$C_\alpha$ bond (**7c**). This non-agostic conformation lies only +28 kJ/mol above **5**, indicating that **7d** and **7e** are not stable conformations since they are higher in energy. However, **7** can stabilize itself by a simple rotation about the Pd−$C_\alpha$ bond, establishing a $\eta^2$-interaction between the carbonyl group and the Pd atom. The relaxation from **7c** to **7a** has no intervening barrier and is therefore a spontaneous reaction. The change from $\beta$-agostic (**7b**) to $\eta^2$-carbonylic conformation (**7a**) yields −31 kJ/mol, making the overall step **5** → **7a** exothermic by −12 kJ/mol. The strength of the $\eta^2$-bond in **7a** can be estimated to be 40 kJ/mol from the energy difference between **7c** (which has a $\eta^1$-carbonyl conformation without agostic bonds) and **7a**.

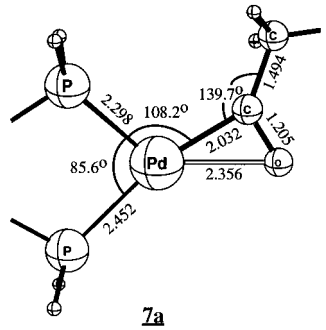


**7a**

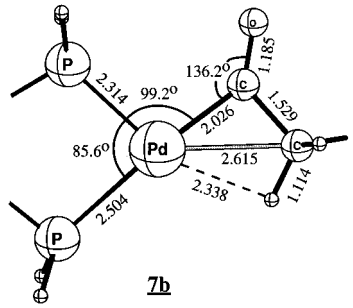


**7b**

To propagate the chain, **7** can take up free olefin, which is subsequently inserted into the Pd−carbonyl bond of the acyl. Geometry optimization reveals that coordination of ethylene to one of the free apical positions (**8**) leads directly to a square-planar coordination (**9**) with the ethylene occupying the

(31) Margl, P.; Ziegler, T.; Blöchl, P. E. *J. Am. Chem. Soc.* **1995**, *117*, 12625.
(32) Ziegler, T.; Tschinke, V.; Ursenbach, C. *J. Am. Chem. Soc.* **1987**, *109*, 4825.
(33) Ziegler, T.; Versluis, L.; Tschinke, V. *J. Am. Chem. Soc.* **1986**, *108*, 612.
(34) Ziegler, T. *Chem. Rev.* **1991**, *91*, 651.
(35) Margl, P. M.; Ziegler, T.; Blöchl, P. E. *J. Am. Chem. Soc.* In press.
(36) Koga, N.; Morokuma, K. *Chem. Rev.* **1991**, *91*, 823.

coordination site vacated by removal of $\eta^2$-interaction. The potential well associated with rotation of the ethylene moiety about the ethylene−Pd bond in **9** is extremely shallow. We calculate the variation of the total energy with respect to rotation about the Pd−ethylene bond to ≈5 kJ/mol, due to the basic invariance of overlap between ethylene $\pi^*$ orbitals and metal-based d orbitals. The preference for out-of-plane arrangement of the olefin ligand is due to reduction of steric hindrance in the molecular plane. We note that the perfect out-of-plane arrangement of the acyl ligand is in agreement with previous crystallographic studies on the related complex *cis*-$Pt(PPh_3)_2$-(COPh)(COOMe).[37]

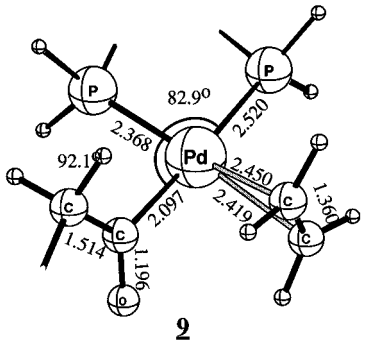


**9**

Insertion of the complexed olefin proceeds by contraction of the distance between the carbonyl carbon and the vicinal olefin carbon. In the early stages of the path from **9** toward the transition state **10**, the carbonyl moiety reorients itself in a manner which ensures optimal stabilizing interaction between the carbon-based $\pi^*_{CO}$ LUMO on the CO group and the occupied $\pi$ orbital on the olefin. As the carbon−carbon distance is further shortened toward **10**, it becomes energetically favorable to reorient the carbon-based $\sigma_{CO}$ orbital on the CO group away from the Pd−acyl bond toward the lobes of the $\pi^*$ LUMO on ethylene, eventually breaking the Pd−acyl bond. Both the $\pi^*_{CO}/\pi_{ethylene}$ and $\sigma_{CO}/\pi^*_{ethylene}$ interactions help stabilize the transition state **10**. Still, the transition state **10** lies 58 kJ/mol above the educt **9**.

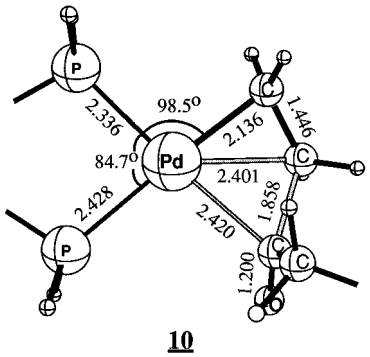


**10**

After the Pd−acyl bond is broken, the carbonyl group is brought into the coordination plane so that the oxygen can interact with the metal center at the vacated site. The chelating oxygen stabilizes **11a** by 104 kJ/mol. This estimate was obtained by comparing the energy of **11a** to that of an optimized structure **11b** in which the CO group is moved away from the Pd by constraining the $Pd-C_\alpha-C_\beta-C_\gamma$ torsion angle to 180°, while minimizing the remaining degrees of freedom. The overall reaction **9** → **11a** was found to be exothermic with an enthalpy of −74 kJ/mol. The geometry for **11a** optimized by our DFT scheme is very close to the structure found by X-ray crystallography for a closely related Pd(II) species, namely $Pd(PPh_3)_2$(2-acetylnorborn-1-yl)$^+$.[38]

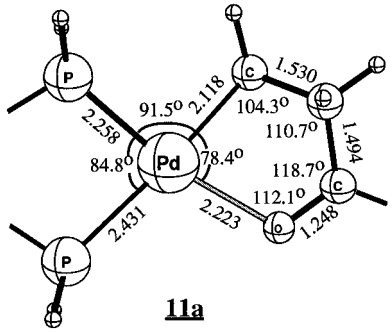


**11a**

Figure 4 underlines that the highest barrier encountered in the productive part of the catalytic cycle is 58 kJ/mol, for the insertion of olefin into the Pd−acyl bond. This is in agreement with previous results,[9] which state that the olefin insertion step is the rate-limiting one in the two-step chain growth sequence. The composition of the resultant polymer, however, will depend on how the energy profile of the productive steps compares with the energy profiles for the misinsertion steps. In the next sections, we will compare the energetics of olefin and CO double insertions to explain the predominant formation of alternating copolymers.

**(b) CO Double Insertion.** A misinsertion of CO into the growing polymer chain would lead to the formation of a ketoacyl segment. This can be envisioned as a branch from the productive part of the reaction, taking place by uptake of a CO molecule instead of an olefin by **7** (Figures 2 and 5). Uptake of CO into the free apical position of **7a** (**7b**) leads without any intermittent energy maximum to the square-planar structure **14**, in which the acyl chain has lost all agostic bonding to palladium. The exothermicity of the CO uptake step is −78 kJ/mol, which is in the range expected. We note that uptake of ethylene (**7a** + $C_2H_4$ → **9**) in the productive step, which is a rivaling reaction (Figure 4), is less exothermic with $\Delta H_{7-9} = -55$ kJ/mol.

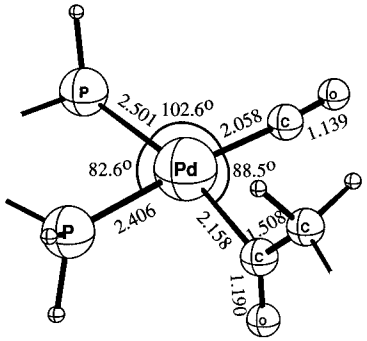


**14**

The migratory insertion of CO into a $M^{II}$−acyl bond has been studied experimentally by Sen et al.[37] for M = Pt and Pd. It has been concluded that the process is thermodynamically unfavorable.[39] We find that the transition state **15** occurs at a late stage, where the acyl−Pd bond has already been broken (Pd−C(acyl) distance ≈ 3 Å), which is to be expected for an endothermic reaction (Figure 5). It is interesting to note that the formation of **15** involves two rotations: (a) An incipient rotation about the $C_\alpha-C_\beta$ bond, which leads eventually to a stabilization of the product by chelation of the Pd atom and an

(37) Sen, A.; Chen, J.-T.; Vetter, W. M.; Whittle, R. R. *J. Am. Chem. Soc.* **1987**, *109*, 148.

(38) Brumbaugh, J. S.; Whittle, R. R.; Parvez, M.; Sen, A. *Organometallics* **1990**, *9*, 1735.

(39) Chen, J.-T.; Sen, A. *J. Am. Chem. Soc.* **1984**, *106*, 1506.

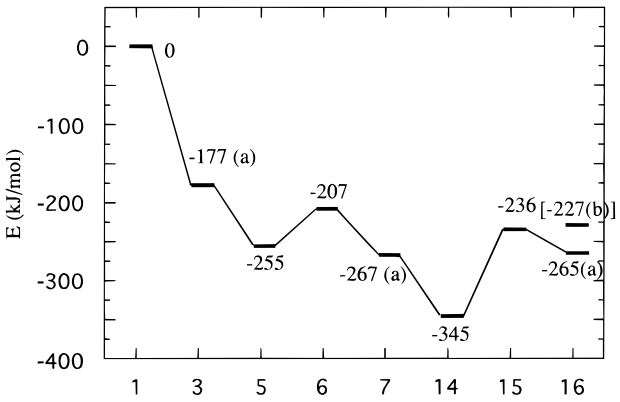


**Figure 5.** Energy profile for the CO double insertion reaction. Units and conventions as in Figure 4. For clarity, the section of the productive cycle immediately preceding CO misinsertion is also shown (**1**−**7**).

energetic stabilization by establishing $\pi$-bond conjugation between the carbonyl groups, and (b) a rotation about the Pd−$C_\alpha$ bond which actually moves the $\beta$-carbonyl away from the metal. Whereas (a) is readily attributed to the favorable energetics of a conjugated $\pi$-system and to reduction of Coulomb repulsion between the oxygen atoms, (b) is counter intuitive in the way that it actually weakens a possible chelate bond between oxygen and Pd. However, the potential well for the latter degree of freedom is extremely shallow, permitting rotations of ±10° with a change of less than 1 kJ/mol of the total energy. In view of this fact a detailed discussion of this effect cannot be regarded as useful.

The transition state **15** lies 109 kJ/mol above the educt **14**. Thus, the nonproductive insertion of CO into **7** (Figure 5) has a higher barrier than the productive insertion of ethylene (Figure 4), with barrier of +58 kJ/mol. The higher barrier stems from the ability of a late transition metal such as palladium to form stronger bonds to CO (as in **14**) than to ethylene (as in **9**). Furthermore, the transition state **15** (CO misinsertion) is seen to lie 28 kJ/mol (Figure 5) above the transition state **10** (productive ethylene insertion, Figure 4).

The overall reaction **14** → **16a** is strongly endothermic by 80 kJ/mol. We attribute the unfavorable energetics of the reaction to the following: (a) loss of a strong $\pi$-acceptor (CO) at the Pd center, (b) a weak (O)C−C(O) bond in comparison to the (O)C−$C_2H_5$ linkage, and (c) a weaker stabilization of the product by chelate bonding of oxygen. Comparison with the barriers for alternating insertion shows that the CO double insertion is clearly unfavorable due to an excessively high barrier (**9** → **10**: +58 kJ/mol; **14** → **15**: +109 kJ/mol) for the insertion of the second carbon monoxide and an adverse thermodynamic driving force (**7a** + $C_2H_4$ → **11a**: −129 kJ/mol; **7a** + CO → **16a**: +2 kJ/mol). Therefore, it is clear that CO double insertion cannot be considered to compete with the productive steps.

**(c) Olefin Double Insertion.** We model the double insertion of olefin into the polymer chain as shown in Figure 3. The misinsertion can be seen as a branching from the productive cycle originating from **3**. At this stage it is decided whether a path of alternating copolymerization or olefin double insertion is followed. If **3** takes up a CO molecule, an alternating copolymer will be created. If **3** takes up an olefin, a butyl segment will be inserted into the growing chain. The reaction steps discussed in this chapter have already been investigated in a study by Ziegler et al.[30] dealing with ethylene oligomerization by a similar Ni system.

Uptake of olefin into the free apical position of **3a** (or **3b**) leads directly to the square-planar $\pi$-complex **18**, since the 5-coordinate square-pyramid **17** is not a stationary structure.

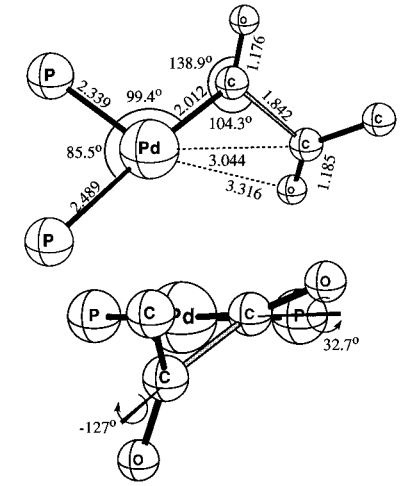


**15**

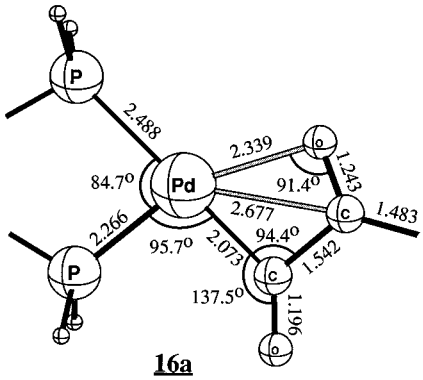


**16a**

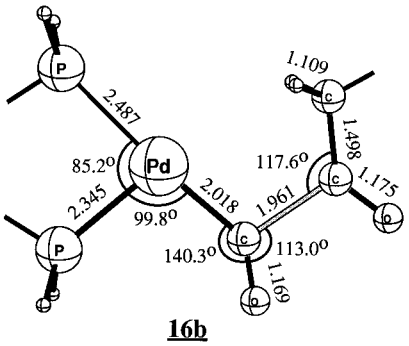


**16b**

As in **9**, the ethylene moiety in **18** is mobile with respect to rotation around the Pd−ethylene bond. The total energy of **18** changes less than 5 kJ/mol with respect to rotation of $C_2H_4$ around this axis and as in **9**, the out-of-plane arrangement is favored because of reduced steric repulsion. The exothermicity of the ethylene uptake step is −51 kJ/mol (Figure 6). Thus, the unproductive ethylene uptake by **3a** is less favorable than the corresponding productive CO addition, which has an exothermicity of −78 kJ/mol. We note that the CO and $C_2H_4$ uptake energies of **7a** and **3a** are very similar (**7a** + $C_2H_4$ → **9**: −55 kJ/mol; **3a** + $C_2H_4$ → **18**: −51 kJ/mol; and **3a** + CO → **5**: −78 kJ/mol; **7a** + CO → **14**: −78 kJ/mol). This is in perfect agreement with the fact that the bonds destroyed in the uptake process have about equal strengths (40 kJ/mol for the $\eta^2$-bond of **7a** and 44 kJ/mol for the $\beta$-agostic bond of **3a**).

The insertion of the complexed ethylene into the Pd−ethyl bond proceeds via a transition state geometrically very similar to those encountered in previous studies of Ziegler−Natta catalysis.[40] The transition state **19** is four centered and lies 65 kJ/mol above the $\pi$-complex **18**. By contrast, the rivaling productive CO insertion **5** → **7** has a barrier of only 48 kJ/mol (Figure 4).

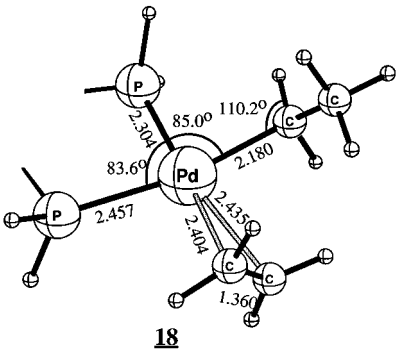


**18**

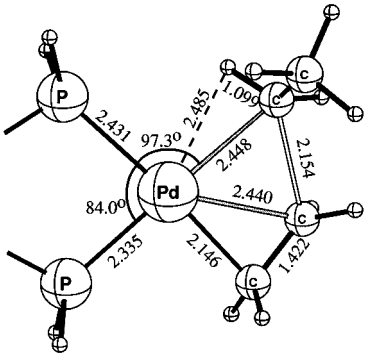


**19**

The high barrier found here for olefin insertion into the $Pd^{II}$−alkyl bond is in stark contrast to the negligible[40,41] activation energy obtained for ethylene insertion into the $M^{IV}$−alkyl bond of group 4 metals in metallocene-catalyzed olefin polymerization. In the group 4 systems, ethylene can use its vacant $\pi^*$ orbital exclusively to form the emerging C−C bond with the α-carbon of the growing chain since back-donation from the electron poor $d^0$ metal center is negligible. By contrast, the $\pi^*$ orbital is involved in back-donation with the electron-rich $d^8$ palladium center in **18** and **19**, and thus is less readily available as an acceptor in the initial bond-forming interaction with the $\sigma$-orbital on the α-carbon of the growing chain.

The primary product of the insertion is the $\gamma$-agostic butyl species **20c**, which lies 17 kJ/mol below **18**. Rearranging the butyl chain into a $\delta$-agostic conformation leads to structure **20b** (21 kJ/mol below **18**), and the most stable conformation is the $\beta$-agostic **20a** (49 kJ/mol below **18**). In all three isomers, the agostic hydrogen occupies one corner of a square-planar configuration. Thus, insertion of ethylene into a Pd−alkyl bond yields exactly −100 kJ/mol. Since the final product **20a** of this insertion is coordinated in the same $\beta$-agostic fashion as **3a**, a third insertion of ethylene would again give exactly −100 kJ/mol. It follows that the exothermicity for the incorporation of a $(C_2H_4)_2$ fragment into the chain is −200 kJ/mol, compared to a value of −219 kJ/mol for the alternating incorporation of CO and $C_2H_4$. So, from the viewpoint of thermodynamic driving force, multiple CO insertions are ruled out completely, whereas the difference between exothermicities of multiple $C_2H_4$ insertions and strictly alternating insertions seems small. However, the barriers encountered in the productive cycle are +48 and +58 kJ/mol, whereas two subsequent $C_2H_4$ insertions face barriers of 65 kJ/mol each.

From the energetics we obtain for insertion of $(C_2H_4)_2$ (−200 kJ/mol) and for $COC_2H_4$ (−219 kJ/mol) it seems that the latter was more favorable on thermodynamic grounds. However, the following calculations

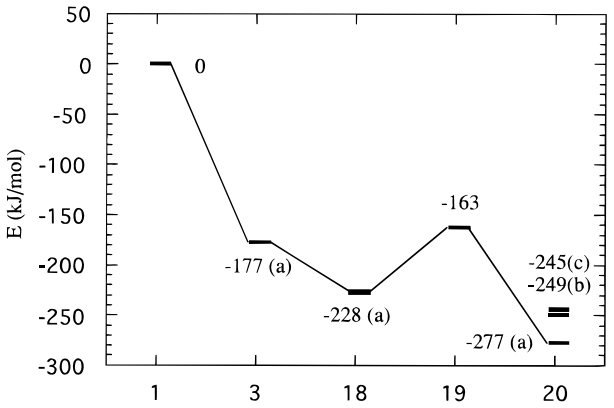


**Figure 6.** Energy profile for the $C_2H_4$ double insertion. Units and conventions as in Figures 4 and 5. For clarity, the section of the productive cycle immediately preceding olefin misinsertion is also shown (**1**−**3**).

$$C_2H_5\text{-}C_2H_5 + C_2H_4 \rightarrow C_2H_5\text{-}C_2H_4\text{-}C_2H_5 \quad \Delta H_{homo} = -92 \text{ kJ/mol}$$

$$C_2H_5\text{-}C_2H_5 + CO \rightarrow C_2H_5\text{-}C(O)\text{-}C_2H_5 \quad \Delta H_{co} = -47 \text{ kJ/mol}$$

reveal that insertion of a $(C_2H_4)_2$ fragment into the chain yields −184 kJ/mol, whereas insertion of $COC_2H_4$ would yield 45 kJ/mol less, namely −139 kJ/mol. A decomposition of the value of −219 kJ/mol shows that it cannot be used directly as an estimate of the thermodynamic driving force for the $COC_2H_4$ insertion, since it contains contributions due to the stabilizations of **3a** and **11a** by their respective chain ends (**3a**: $\beta$-agostic; **11a**: chelate), which are by no means equal (**3a**: −44 kJ/mol; **11a**: −104 kJ/mol). Correcting for this difference of 60 kJ/mol in stabilization yields a value of −159 kJ/mol for the exothermicity of $COC_2H_4$ insertion, which is 41 kJ/mol less than the −200 kJ/mol of $(C_2H_4)_2$ insertion. This agrees nicely with the value of 45 kJ/mol derived from $\Delta H_{homo}$ and $\Delta H_{co}$. In the long run the preference of alternating copolymerization over olefin homopolymerization must therefore be purely kinetic.

To determine the origin of the strong preference for the insertion of an olefin into a Pd−acyl bond over the insertion of CO, we decompose these reactions into

$$C_2H_4 + EtC{=}O^{\bullet} \rightarrow EtC(O)C_2H_4^{\bullet} \quad \Delta H_I = -44 \text{ kJ/mol} \quad \text{(I)}$$

$$EtC(O)C_2H_4^{\bullet} + PdPP^{\bullet+} \rightarrow \mathbf{11a} \quad \Delta H_{II} = -351 \text{ kJ/mol} \quad \text{(II)}$$

$$\mathbf{11a} \rightarrow \mathbf{11b} \qquad \Delta H_{III} = +104 \text{ kJ/mol} \quad \text{(III)}$$

and

$$CO + EtC{=}O^{\bullet} \rightarrow EtC(O)C{=}O^{\bullet} \quad \Delta H_{IV} = -4 \text{ kJ/mol} \quad \text{(IV)}$$

$$EtC(O)C{=}O^{\bullet} + PdPP^{\bullet+} \rightarrow \mathbf{16a} \quad \Delta H_V = -271 \text{ kJ/mol} \quad \text{(V)}$$

$$\mathbf{16a} \rightarrow \mathbf{16b} \quad \Delta H_{VI} = +38 \text{ kJ/mol} \quad \text{(VI)}$$

where we performed spin-unrestricted calculations on fragment geometries created by breaking up the insertion products **11a** and **16a**, while retaining all their geometric parameters. Comparison between eqs I−III and IV−VI allows the breakdown of the total formation energy for **11a** and **16a** into individual contributions arising from individual bonds. Contributions I and IV are directly related to the strength of the C−C bonds formed, steps II and V mirror the total energy gained by forming

(40) Lohrenz, J. C. W.; Woo, T. K.; Ziegler, T. *J. Am. Chem. Soc.* **1995**, *117*, 12793.

(41) Meier, R. J.; vanDormaele, G. H. J.; Iarlori, S.; Buda, F. *J. Am. Chem. Soc.* **1994**, *116*, 7274.

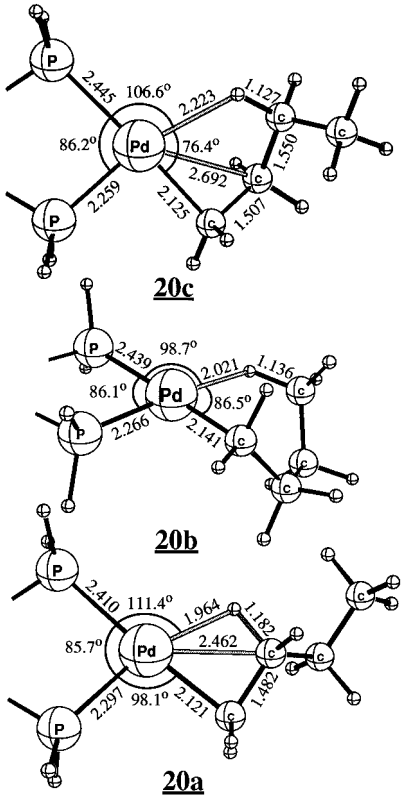


the Pd−C and Pd−O bonds. Steps III and VI give an indication of how much of the total energy gained in steps II and V is due to the formation of the O → Pd bond. From a comparison of $\Delta H_{\mathrm{I}}$ and $\Delta H_{\mathrm{IV}}$ it is obvious that the C−C bond formed between an acyl and CO is much weaker than the C−C bond formed between acyl and ethene. Along the same lines, the addition of the pre-formed chain fragment to the metal center is much less exothermic for the ketoacyl ($\Delta H_{\mathrm{V}}$) than for the ketone ($\Delta H_{\mathrm{II}}$). Subtracting the strength of the chelate bond (which is approximately determined as the energy difference between the chelate species **11a** and **16a** with their respective nonchelating isomers **11b** and **16b**) shows that the chelating bond is much stronger in **11a** than in **16a**. Also, the Pd−C bonds in both systems are of nearly equal strengths (233 kJ/mol in **16a**, 247 kJ/mol in **11a**). It seems, therefore, that the factors responsible for the high energy of **16a** compared to **11a** are the weakness of the chelating and C−C bond, respectively. It is furthermore interesting to note that in **16b**, the C−C bond is opened to 1.961 Å, which is also indicative of the extremely weak C−C bond.

## 4. Conclusion

We have investigated the chain propagation mechanism for alternating copolymerization of CO and $C_2H_4$ by a bis-phosphine Pd(II) catalyst as well as the misinsertions resulting from multiple insertion of olefin and CO, respectively. Our nonlocal density functional calculations allow the following conclusions to be drawn: (i) Strictly alternating copolymerization is kinetically favored over homopolymerization of olefin and thermodynamically as well as kinetically favored over successive multiple insertions of CO. Insertion of one $C_2H_4$−CO unit into the Pd−ethyl bond yields −219 kJ/mol, whereas insertion of a $C_2H_4$−$C_2H_4$ segment yields −200 kJ/mol. Insertion of a CO−CO segment yields only −88 kJ/mol. (ii) Therefore, multiple successive CO insertions are ruled out as competitive side reactions on a thermodynamic basis. (iii) Multiple insertions of $C_2H_4$ are kinetically disfavored compared to strictly alternating copolymerizations. The activation barriers for the insertion of a CO/$C_2H_4$ unit into the chain are only +48 and +58 kJ/mol, respectively, whereas the barrier for $C_2H_4$ insertion is 65 kJ/mol (for each of the two insertions). (iv) Generally, PdPP(acyl)$^+$ species are only weakly stabilized by agostic interactions, whereas the PdPP(alkyl)$^+$ species are strongly stabilized by agostic interactions. The acyl species **7** can stabilize itself by −31 kJ/mol over its most favorable agostic conformation by adopting a $\eta^2$-carbonyl conformation. (v) The growing polyketone chain is strongly stabilized by forming chelate bonds between the carbonyl oxygens and Pd. We estimate a chelate bond strength of −104 kJ/mol for species **11a**. (vi) Summing up, one could say that the number of CO units incorporated into the chain is maximized, because CO (as the better $\pi$ acceptor) stabilizes the reactive center more than ethylene during the adduct formation proceeding insertion and CO also faces a lower barrier during insertion into the chain. On the other hand, subsequent multiple insertions of CO are avoided since they are kinetically as well as thermodynamically highly unfavorable. Olefin homopolymerization is not feasible in the presence of CO since copolymerization is much faster, but it is actually the thermodynamically more favorable process.

The energetics presented in this paper are bound to change slightly as higher-order effects (such as CO/$C_2H_4$ uptake or insertion by a metal center which is stabilized by a chelate bond of the polyketone chain) are taken into account. However, we postulate that these effects will only heighten the preference for alternating insertion found in this study, where only first-order effects of the chain were accounted for. The reasons for this are that there is no possible way the double insertion of CO can be made competitive by higher-order chelating bonds. The only way a misinsertion can happen after ruling out CO misinsertion is that an ethylene unit would insert into a chelate-stabilized chain which is linked to Pd via a $C_2H_4$ unit. However, the chelate bond strengths are in the order of 100 kJ/mol, whereas $C_2H_4$ uptake energies are much smaller (in the order of 50 kJ/mol). Therefore, the incoming $C_2H_4$ is even less likely to displace the chelate bond than it was in the model compound used in the present study (**3a**) to model the misinsertion of ethylene.

**Acknowledgment.** This work has been supported by the National Sciences and Engineering Research Council of Canada (NSERC), as well as by the donors of the Petroleum Research Fund, administered by the American Chemical Society (ACS-PRF No. 20723-AC3). P.M. would like to thank the Austrian Fonds zur Förderung der wissenschaftlichen Forschung (FWF) for financial support within project JO1099-CHE. The authors thank Dr. E. Drent for useful comments on the manuscript.

**Note Added in Proof:** After the submission of the final version of the manuscript, an experimental study on the mechanistic aspects of Pd$^{II}$-catalyzed copolymerization of ethylene and carbon monoxide was published by Rix et al. (*J. Am. Chem. Soc.* **1996**, *118*, 4746) using phenanthroline instead of $PH_2CHCHPH_2$ as a coligand. Their experimentally derived barrier heights match our values closely.

**Supporting Information Available:** Structures of all species mentioned in the text but not displayed, as well as listings of the basis sets used (13 pages). See any current masthead page for ordering and Internet access instructions.

JA960697H